Supplementary Information for Chapter 3

Supplementary Methods

Histological sampling

In order to preserve the original morphology of the elements sampled, we molded all elements using Smooth-On Mold Star Series platinum silicon rubber, then created casts with these molds using Smooth-On Smooth Cast 300 (www.smooth-on.com), as well as photographing the elements to be sampled. After this, we embedded the elements to be sectioned in Castolite AC polyester resin (www.eagerplastics.com). After the resin had cured, we cut 1.5-mm thin wafers of cross sections of the element with a Buehler Isomet 1000 precision saw with a diamond-bladed sawblade. In order to examine the most complete record of life history possible, we cut the rib fragments perpendicular to the proximal-distal axis, and the fibula was cut in the same way as close to the center of the bone as available. The wafers were ground and polished on one side with a Buehler Ecomet III grinder/polisher, using progressively finer grinding paper (1200–2400 grit) before polishing with 0.3-micron polishing slurry. The wafer was then glued polished side down onto a plastic microscope slide (thickness ~1 cm) with Loctite cyanoacrylate glue. The other side of the wafer was then ground and polished in the same way until thin enough to observe relevant histological details under a microscope. We used an Olympus BX51 microscope to observe the histological slides, and captured images with a Lumenera Infinity 1 digital camera for miscroscopes.

Supplementary Description

NMMNH P-4563 (fibula) histological description

The osteohistology of this element is highly unusual and difficult to interpret fully, although the histology strongly indicates that this individual was still growing rapidly at the time of death. The internal portion of the cortical bone, closest to the medullary cavity, is comprised of woven bone arranged in a fibrolamellar complex, and is highly vascularized throughout in a combination of longitudinal and reticular orientation (sensu Huttenlocker et al. 2013). There is no line of arrested growth (LAG) within this portion of the cortex; however, a thin (20–40 μm) band of lighter bone resembling an annulus is present in this section. However, this band is not traceable around the entirety of the cortex and is as strongly vascularized as the bone immediately surrounding it, suggesting that this feature is not an annulus.

This 'normal' cortical bone is interrupted by a LAG (although in some areas this LAG transitions to an annulus of osteocyte-dense, avascular bone), which seperates the deeper 'normal' bone from the highly unusual superficial bone, which is retained for much of the cortex until just deep to the subperiosteal surface. This bone is woven-fibered and highly vascular, but unlike the deeper cortical bone, lamellar bone has been circumferentially deposited in the vascular cavities to form osteons. Because of this, the vascular cavities are extremely large with respect to those of the normal bone of the deeper cortex, giving the bone of this region a porous appearance. These large vascular canals are primarily radial in orientation. Osteocyte lacunae are larger and denser in this region than in the normal fibrolamellar bone of the deeper cortex. In some portions, most notably in the posterior portion of this region, this bone is so porous that it resembles cancellous or spongy bone. Strangely, in a few limited areas this high vascular, porous bone

'invades' the deeper fibrolamellar bone. In these places, the LAG/annulus is truncated by the highly vascular bone, which extends deeper into the bone to the medullary cavity. The highly vascular bone is distinctly separated from the surrounding fibrolamellar bone by structures analogous to cement lines of secondary bone (although this is not secondary bone). The medullary cavity is bordered by avascular, compact lamellar bone, but in some areas the highly vascular bone extends all the way into the medullary cavity, truncating the lamellar bone that acts as a boundary. In these regions, another layer of compact lamellar bone has been deposited, separating the highly vascular bone from the medullary cavity. Some cortical drift of the medullary cavity has occurred, as evidenced by truncated 'normal' cortical bone. In the exteriormost portions of the corex, directly beneath the subperiosteal surface, the highly vascular tissue transitions into woven bone in a fibrolamellar complex with plexiform- or reticular-style vascularization. The tissue remains highly vascularized to the subperiosteal surface, and there is no external fundamental system (EFS). There is no evidence of remodeling or secondary bone in this specimen. Despite the unusual histology of this individual, which may be related to some pathology or unusual feature of this individual's biology, all evidence suggests that this individual had not ceased or slowed growth at the time of death, and was probably still growing rapidly.

NMMNH P-4569 (rib fragments) histological description

The smaller rib fragment (NMMNH P-4569, slide 1) is mostly cortex, with the rest of the rib missing. The interiormost portion of the bone is comprised of vascular, loosely woven bone with no primary osteons, and is bordered interiorly by

avascular lamellar bone that presumably forms the border of the medullary cavity. This loosely woven bone transitions to woven bone with primary some large primary osteons spaced further apart than is typical for woven bone in a fibrolamellar complex. The vascular canals in these osteons are large and longitudinally oriented, and this region of the bone remains highly vascular. From this region the bone transitions smoothly into more typical fibrolamellar bone, with reticular and longitudinal vascular canals predominating, and this tissue takes up the majority of the surface area of the histological section. Although the vascular canals are larger in the interior tissues than in the more typical fibrolamellar bone, they are far denser in the more external bone tissues. A few visually distinct, circumferential linear structures are present in the cortex, but these are not traceable or continuous across the entire cortex, and appear to only be present in certain sections. There are no LAGs or annuli, and the bone tissue remains strongly vascularized to the subperiosteal surface.

Unlike slide 1, the rib fragment of NMMNH P-4569 sampled for slide 2 enables the complete cross-sectional area of the rib to be examined. The internal portion of the rib is composed of cancellous bone, and this tissue extends to the subperiosteal surface on the medial side of the rib. In the lateral, anterior, and posterior portions it transitions into well-vascularized woven bone in fibrolamellar complex smoothly, with no lamellar bone or LAG interrupting the transition. The vascularization style is longitudinal throughout, and the level of vascularization is consistent between interior and exterior cortical bone, although the vascular canals tend t be slightly larger in the interiormost portion of the cortical bone. There are no

LAGs or annuli present, and there has been no remodeling so secondary osteons are absent. The bone is vascularized up to the subperiosteal surface, but the first ~200 μm of bone directly underlying the subperiosteal surface appears to be less vascularized. There is no EFS present in the subperiosteal surface. Although the slightly lower amount of vascularization in the externalmost portion of the cortex may suggest that growth has slowed somewhat relative to the rate of earlier bone deposition, growth is still occurring fairly rapidly in this individual, consistent with the histological signal from the same individual in slide 1 of this specimen. The slightly different signal with respect to vascularization of the tissue immediately beneath the subperiosteal surface may reflect differences in where on the rib the fragments originated.

Table S1. Measurements and geological ages/dates for taxa described in this study.

Taxon	Specimen Number	Element measured	Length (mm)	Source
Gojirasaurus quayi	UCM 47721	Tibia, proximodistal length	463	Measured in person
Liliensternus liliensterni	HMN MB.R.2175	Femur, proximodistal length	424	Benson et al. 2014
Zupaysaurus rougieri	PULR-076	Skull length	">38 cm, 60% that of *Dilophosaurus*"	Benson et al. 2014
Bull Canyon Neotheropod	NMMNH P-4569	Femur, maximum length of femoral head	63.02	Measured in person
N/A	NMMNH P-4563	Fibula, anteroposterior length of proximal end	59.43	Measured in person
Herrarasaurus ischigualastensis	PVL 2566	Femur, proximodistal length	482	Benson et al. 2014

Equivalent measurement in *Dilophosaurus* (mm)	Source	Geological Formation	Geological age (Ma)	Source
538.77	A. Marsh, pers. comm.	Bull Canyon Fm. (= Cooper Canyon Fm.), USA	213–208	Bull Canyon Fm. is Revueltian (Lucas and Hunt 1993) and Norian (228-208 Ma). The Adamanian-Revueltian boundary has been dated between 219-213 Ma
557.46	A. Marsh, pers. comm.	Trossingen Fm., Germany	228–208	Norian (Rauhut and Hungerbühler 1998)
N/A	Benson et al., 2014	Los Colorados Fm., Argentina	227–213	Kent et al. 2014
111.16	A. Marsh, pers. comm.	Bull Canyon Fm., USA	213–208	See Bull Canyon Fm. above
89.84 (averaged between left and right elements)	A. Marsh, pers. comm.	Bull Canyon Fm., USA	213–208	See Bull Canyon Fm. above
557.46	A. Marsh, pers. comm.	Ischigualasto Fm., Argentina	231–225	Martínez et al. 2011

References

Benson, R. B. J., N. E. Campione, M. T. Carrano, P. D. Mannion, C. Sullivan, P. Upchurch, and D. C. Evans. 2014. Rates of dinosaur body mass evolution indicate 170 million years of sustained ecological innovation on the avian stem lineage. PLoS Biology 12:e1001853.

Huttenlocker, A. K., H. Woodward, and B. K. Hall. 2013. The biology of bone; pp. 13–34 *i*n K. Padian, and E.-T. Lamm (eds.), Bone Histology of Fossil Tetrapods: Advancing Methods, Analysis, and Interpretation. University of California Press, Berkeley, CA.

Lucas, S. G., and A. P. Hunt. 1993. Tetrapod biochronology of the Chinle Group (Upper Triassic), western United States. New Mexico Museum of Natural History and Science Bulletin 3:327–329.

Martínez, R. N., P. C. Sereno, O. A. Alcober, C. E. Colombi, P. R. Renne, I. P. Montañez, and B. S. Currie. 2011. A basal dinosaur from the dawn of the dinosaur era in southwestern Pangaea. Science 331:206–210.

Rauhut, O. W. M., and A. Hungerbühler. 1998. A review of European Triassic theropods. Gaia 15:75–88.

Figure S1. Elements of *Gojirasaurus quayi* (UCM 47721) showing ontogenetic character states from Chapter 1, Chapter 2. **A** Proximal end of the left tibia in medial view. **B** Distal end of the left tibia in posterior view. **C** A sacral vertebra (either sacral 1, 2, or 3) in left lateral view. **D** Distal end of right scapula in medial view. **E** Proximal end of left pubis in lateral view. All scale bars represent 1 cm.

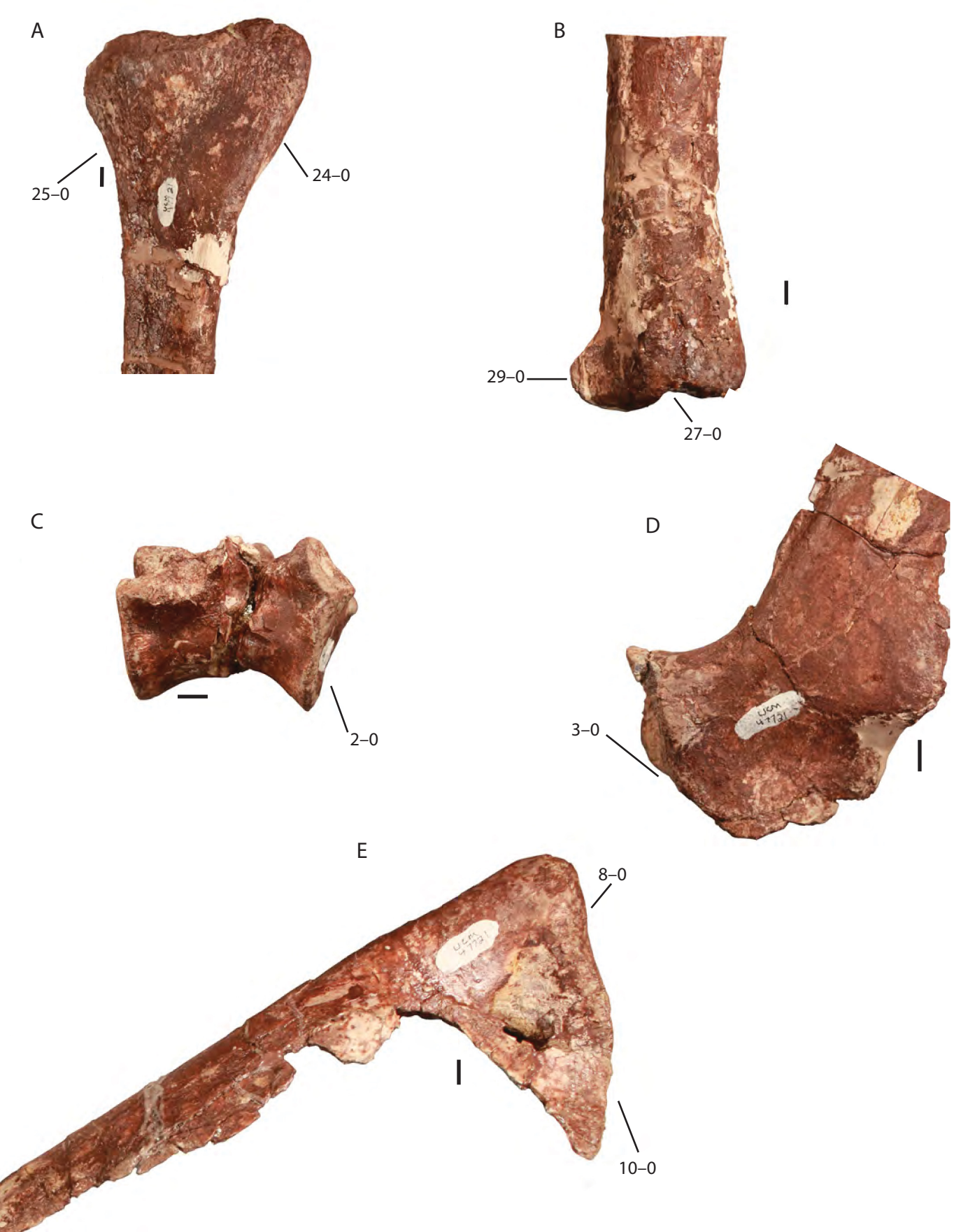
A
25–0
24–0
B
29–0
27–0
C
2–0
D
3–0
E
8–0
10–0

Figure S2. Axial, forelimb, and pelvic elements of *Liliensternus liliensterni* (HMN MB.R.2175) showing ontogenetic character states from Chapter 1, Chapter 2. Note that at least two individuals form this specimen. **A** Sacral vertebrae in left lateral view. **B** Right ilium in lateral view. **C** Proximal end of right pubis in lateral view. **D** Proximal end of right ischium in lateral view. **E** Distal end of right scapula in medial view. **F** Right scapulocoracoid in medial view. **G** Right humerus in lateral view. All scale bars represent 1 cm.

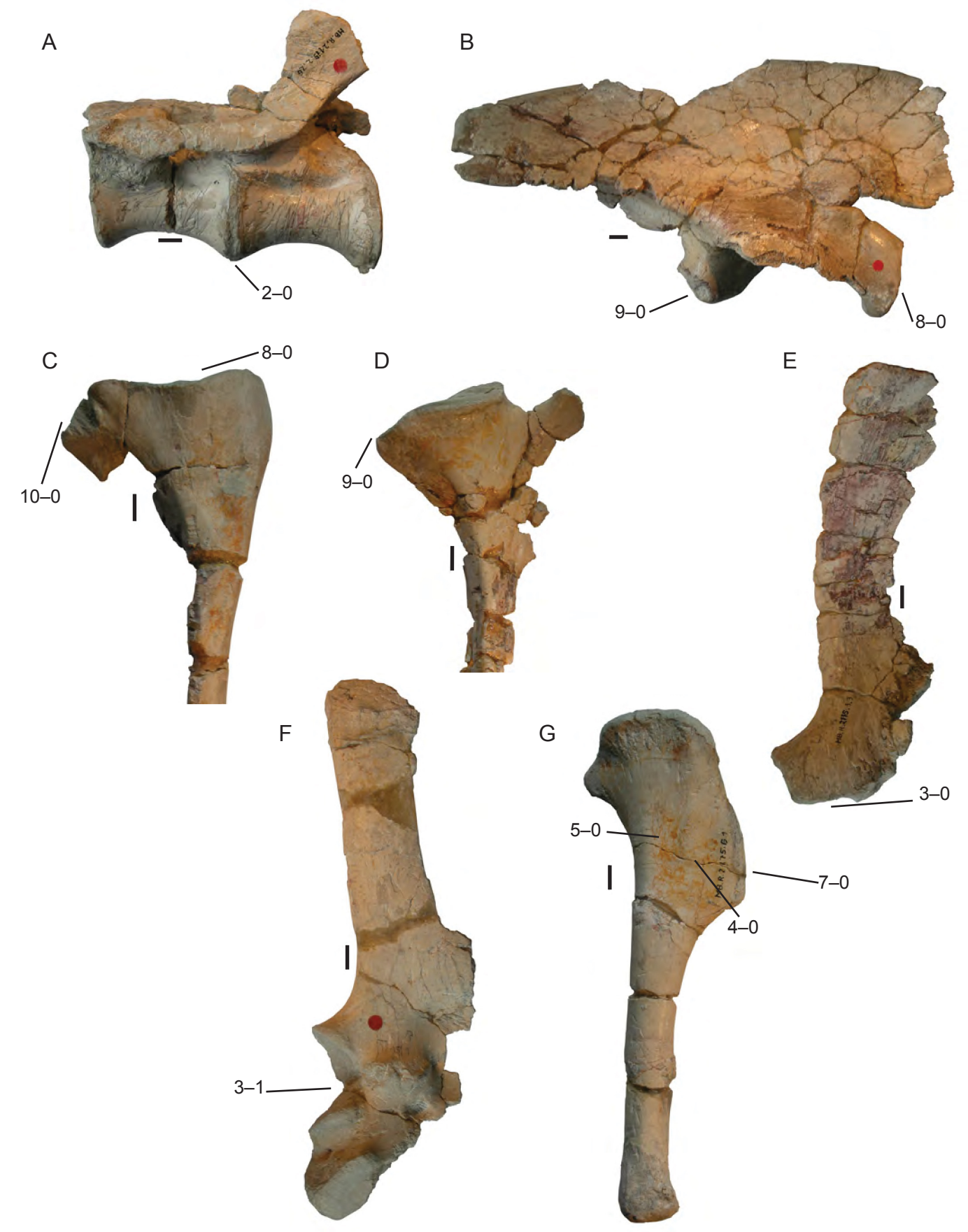
A
2–0
B
9–0
8–0
C
8–0
10–0
D
9–0
E
3–0
F
3–1
G
5–0
7–0
4–0

Figure S3. Hindlimb elements of *Liliensternus liliensterni* (HMN MB.R.2175) showing ontogenetic character states from Chapter 1, Chapter 2. Note that at least two individuals form this specimen. **A** Proximal end of right femur in anterolateral view. **B** Proximal end of right femur in proximal view. **C** Proximal end of left femur in posteromedial view. **D** Proximal end of left tibia in medial view. **E** distal end of right tibia in anterior view. **F** Right astragalus and calcaneum in anterior view. **G** Left metatarsal II in anterior view. All scale bars represent 1 cm.

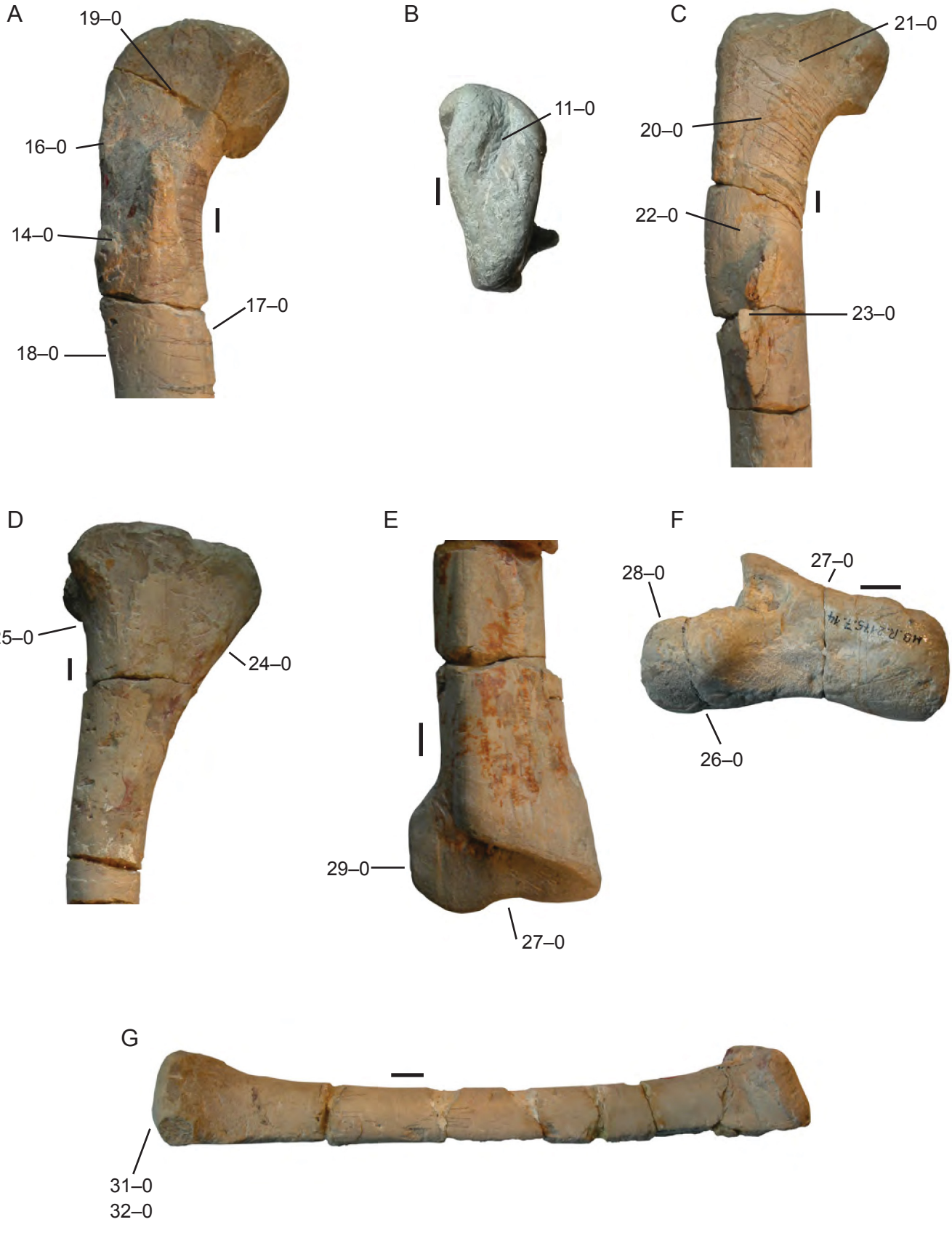
A
19–0
16–0
14–0
17–0
18–0
B
11–0
C
21–0
20–0
22–0
23–0
D
25–0
24–0
E
29–0
27–0
F
28–0
27–0
26–0
G
31–0
32–0

Figure S4. Elements of the Bull Canyon neotheropod (NMMNH P-4569) and the isolated neotheropod fibula (NMMNH P-4563) showing ontogenetic character states from Chapter 1, Chapter 2. **A** Pubic peduncle of right ilium in medial view. **B** Pubic peduncle of right ilium in ventral view. **C** Distal end of left scapula in lateral view. **D** Proximal end of left femur in anterolateral view. **E** Proximal end of left femur in proximal view. **F** Proximal end of left femur in posteromedial view. **G** Partially fused left astragalus and calcaneum in posterior view. **H** Left fibula of a large neotheropod (NMMNH P-4563) in medial view.

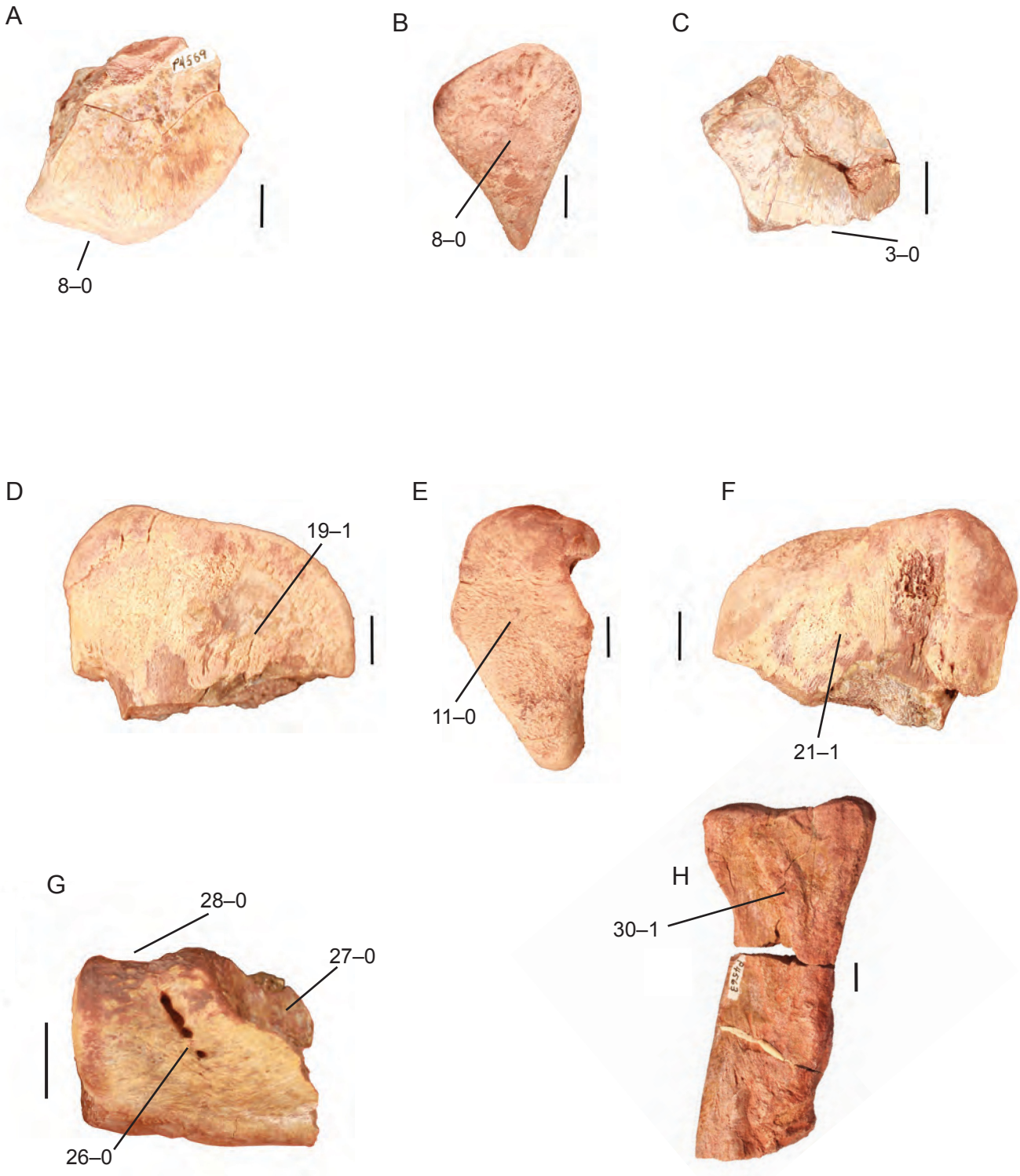
A
8–0
B
8–0
C
3–0
D
19–1
E
11–0
F
21–1
G
28–0
27–0
26–0
H
30–1

Figure S5. Ontogenetic character states of large-bodied Triassic theropods with the range of order in ontogenetic sequences that these characters transition from immature to mature state in *Coelophysis bauri*. Although there is a large amount of variation in the order in which these ontogenetic characters transition states, in *C. bauri* many characters transition consistently earlier or later in ontogeny, allowing the ontogenetic stage of closely related theropods to be estimated based on suites of character states. Red boxes indicate characters that are scored as immature (providing an upper bound on ontogenetic stage), yellow boxes indicate characters that are scored as mature (providing a lower bound on ontogenetic stage), and white boxes indicate characters that could not be scored. The light red region indicates the ontogenetic stages that are consistent with the character states. **A** Character states for *Gojirasaurus quayi* (UCM 47721). **B** Character states for *Zupaysaurus rougieri* (PULR-076). **C** Character states for *Liliensternus liliensterni* (HMN MB.R.2175). Note that multiple individuals make up this specimen: the box containing both yellow and red indicates the scapulocoracoid, which is mature in one individual in the specimen but immature in another.

A

Gojirasaurus quayi

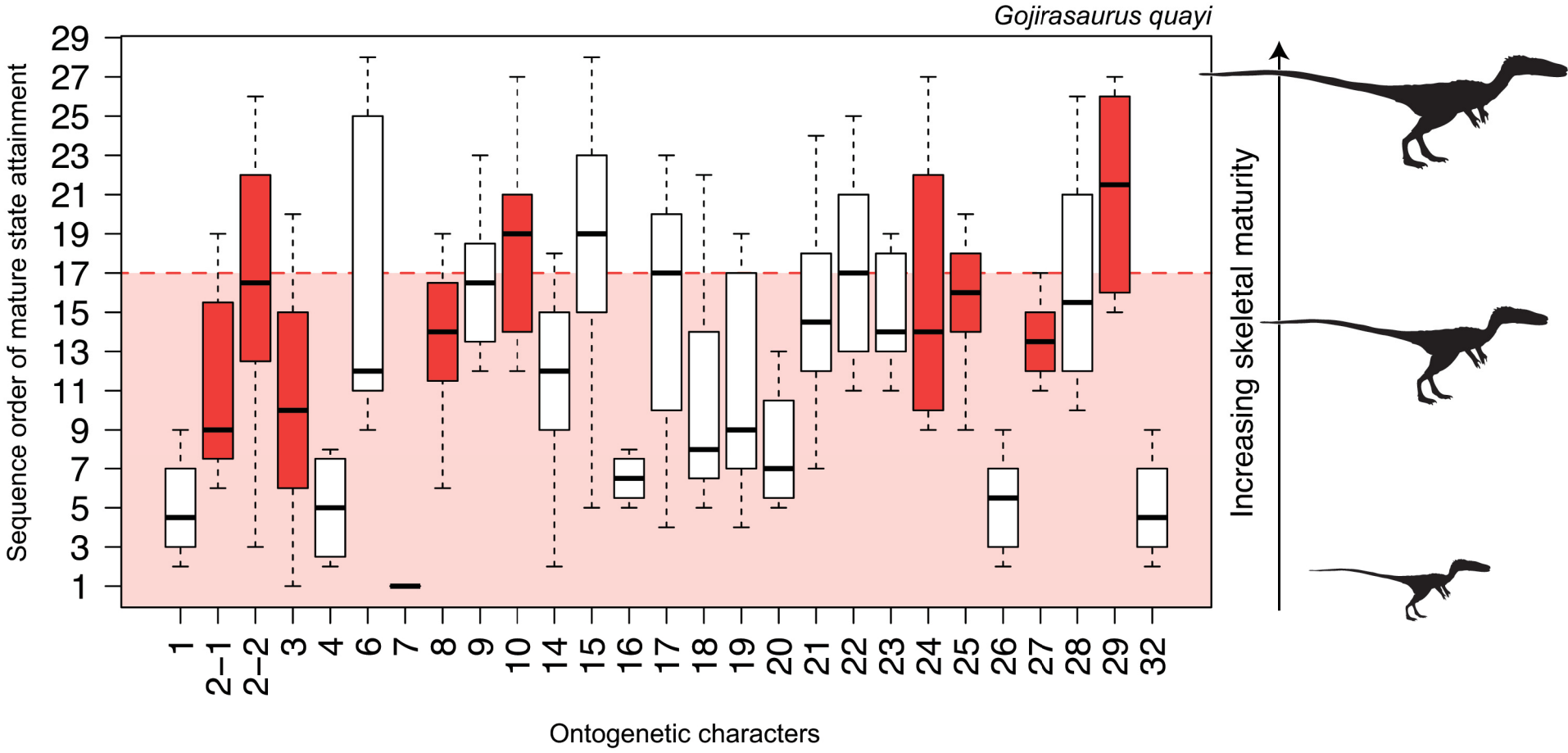

B

Zupaysaurus rougieri

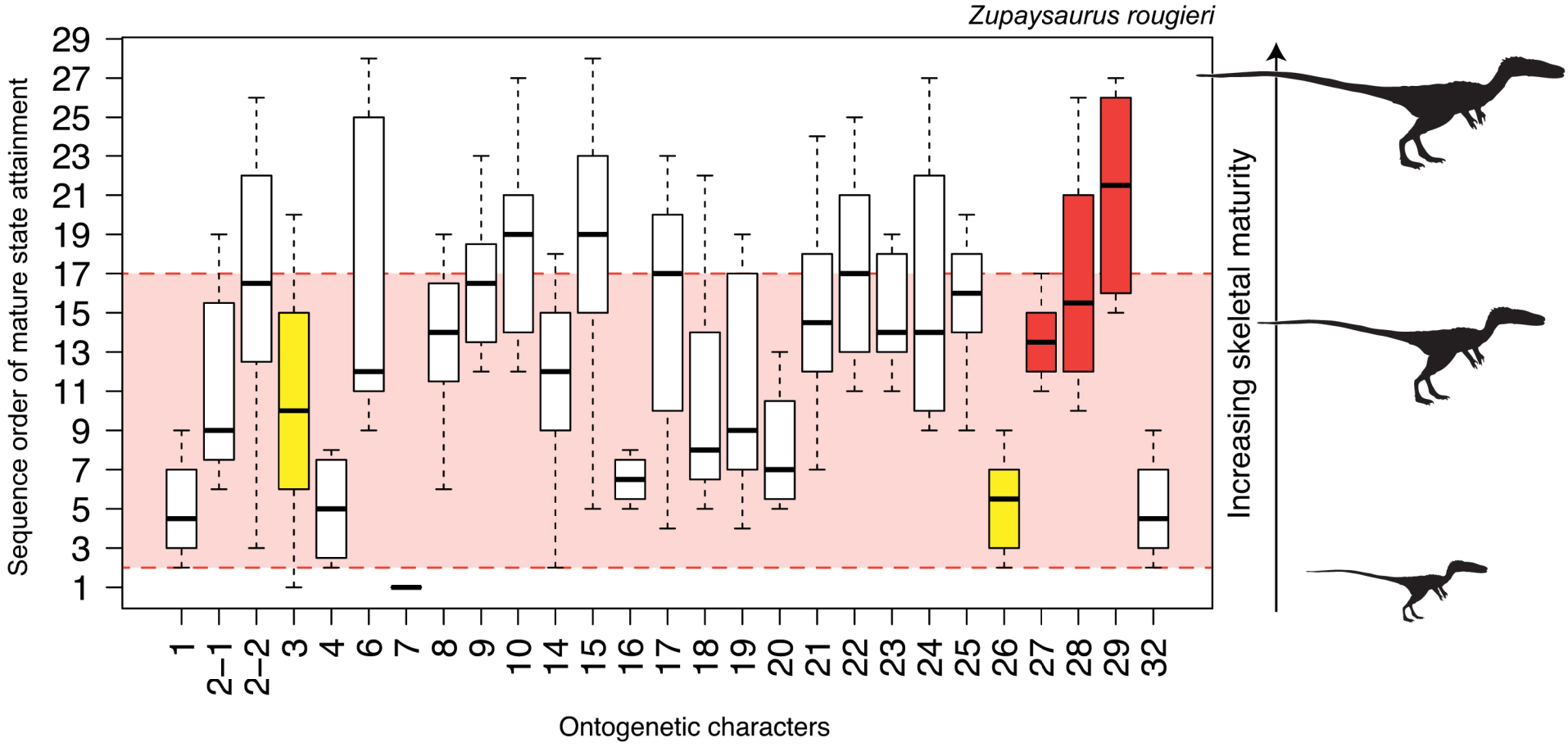

C

Liliensternus liliensterni